

Student Name: Hilary Bews**Date:** 08/07/2015**Project Title:** The cardioprotective role of NACA in the prevention of Doxorubicin and Trastuzumab mediated cardiotoxicity**Primary Supervisor Name and Department:**

Dr. Davinder Jassal; Section of Cardiology, Department of Internal Medicine

Co-Supervisor Name and Department:**SUMMARY: (no more than 250 words single spaced)**

Breast cancer is a significant public health concern, exhibiting both high incidence and mortality rates. Anthracyclines, including Doxorubicin (DOX), constitute the mainstay of breast cancer therapy in both the adjuvant and metastatic settings, but are associated with an increased risk of cardiotoxicity. The coadministration of monoclonal antibodies, such as Trastuzumab (TRZ) further potentiates the cardiotoxicity associated with DOX. The central role of oxidative stress (OS) in the pathophysiology of DOX+TRZ mediated cardiotoxicity warrants investigating whether or not anti-oxidants can serve as cardioprotective agents by interfering with this process. Recently, *in vitro* studies have evaluated a cardioprotective role for the anti-oxidant N-acetylcysteine amide (NACA) in preventing DOX mediated cardiac damage. The purpose of this study to investigate the potential cardioprotective role of NACA in an *in vivo* model of DOX+TRZ mediated cardiotoxicity. A total of 100 C57Bl/6 female mice were randomized to receive: (1) Saline; (2) NACA; (3) DOX; (4) TRZ; (5) DOX+TRZ; (6) NACA+DOX; (7) NACA+TRZ; and (8) NACA+DOX+TRZ. Echocardiography was conducted serially for 10 days, after which mice were euthanized for histological and biochemical analyses. Prophylactic NACA was partially cardioprotective against DOX+TRZ mediated cardiotoxicity by attenuating: i) adverse cardiovascular remodelling as assessed by echocardiography; ii) histological changes consistent with cardiac architectural remodelling; iii) OS, as quantified by lipid peroxidation and superoxide production; and iv) apoptosis, as quantified by caspase-3 and Bax/Bcl-xL. In the future, we will translate these basic science findings into the clinical arena in order to decrease the burden of cardiovascular disease in the breast cancer population.

**Student Signature****Supervisor Signature****ACKNOWLEDGEMENTS:**

I gratefully acknowledge the support by one or more of the following sponsors;

CancerCare MB

H.T. Thorlakson Foundation

Dean, College of Medicine

Research Manitoba

Children's Hospital Research Institute of MB

Kidney Foundation of Manitoba

Manitoba Medical Service Foundation

Associate Dean (Research), College of
Medicine

Heart and Stroke Foundation

Health Sciences Centre Research
Foundation

Other: CIHR, Dr. James Pullar Memorial Trust

INTRODUCTION

For decades, breast cancer has remained the most common cause of cancer and the second most common cause of cancer related deaths in Canadian females.¹ In 2015 alone, 25 200 Canadians were diagnosed with breast cancer, and 5 100 deaths were attributed to the disease.¹ Furthermore, 1 in 9 females will develop breast cancer over their lifetime, illustrating the significant burden that breast cancer places on public health.¹

Breast cancer treatment is multifaceted, including the local modalities of surgical resection and radiotherapy, as well as systemic treatments including chemotherapy, hormone therapy, and biological therapies. Anthracyclines, including doxorubicin (DOX) and epirubicin, have repeatedly demonstrated survival benefits in both the adjuvant and metastatic settings of breast cancer.^{2,3} As such, anthracyclines constitute the mainstay of chemotherapeutic treatments in the breast cancer setting and are typically administered as cocktails, namely adriamycin-cyclophosphamide (AC) and 5-fluorouracil-epirubicin-cyclophosphamide (FEC). Despite the beneficial anti-tumor activity of DOX in the breast cancer setting, the inherent cardiotoxicity associated with this anti-cancer drug limits its therapeutic use. DOX is known to be cardiotoxic at cumulative doses exceeding 550 mg/m², a concentration which has emerged as an absolute upper ceiling for treatment.^{4,5} Furthermore, DOX mediated cardiotoxicity is dose dependent and increases to an incidence of >30% at cumulative doses greater than 600 mg/m².⁵ DOX mediated cardiotoxicity may occur at even lower cumulative doses in patients with the following risk factors including age >70 years, pre-existing heart disease, and previous or concurrent radiotherapy.^{4,6} DOX induced cardiomyopathy is associated with a poor prognosis, with mortality rates as high as 61%, and is typically refractory to conventional anti-heart failure therapy.⁷

More recently, targeted biological therapies were developed in the breast cancer setting to antagonize the human epidermal growth factor receptor 2 (HER-2), a tyrosine kinase receptor responsible for cellular growth, differentiation, and survival. Analysis of breast cancer tissues has demonstrated HER-2 to be overexpressed in 25-30% of malignancies.⁸ HER-2 overexpression predicts shortened overall survival and time to relapse, and is associated with greater axillary lymph node involvement.⁸ A recombinant monoclonal antibody, Trastuzumab (TRZ), was developed in the 1990's to antagonize the extracellular domain of the HER-2 receptor.⁹ A number of multicentre randomized control trials have evaluated the efficacy of TRZ as an adjunct to standard chemotherapy in HER-2 positive breast cancer.⁹⁻¹⁰ These trials demonstrated an overall survival advantage of up to 37% for patients in the TRZ treatment arm. Furthermore, TRZ has been validated as first line treatment for HER-2 positive metastatic breast cancer.¹¹ Despite its widespread adoption, TRZ potentiates DOX mediated cardiotoxicity. In 2007, a retrospective study conducted at CancerCare Manitoba by our group demonstrated that approximately 1 in 4 women administered TRZ therapy as an adjuvant to anthracycline based chemotherapy developed cardiotoxicity.¹² Currently, there exists no approved clinical therapy to prevent the cardiotoxic side effects of DOX+TRZ therapy in both the adjuvant and metastatic settings of breast cancer. As such, the development of strategies to mitigate DOX+TRZ mediated cardiotoxicity, while at the same time maintaining the anti-cancer effects of the two drugs, is important to decrease morbidity and mortality in the breast cancer population.

Amongst the number of mechanisms associated with DOX+TRZ mediated cardiotoxicity, increased oxidative stress (OS) has been the focus in recent years. DOX can catalyze the formation of superoxide radicals from molecular oxygen.¹³ The issue is further compounded by the concomitant depletion of cytosolic glutathione (GSH) peroxidase, and thus cellular anti-oxidant reserve.^{7,13} OS induces phosphorylation and subsequent activation of mitogen-activated

protein kinases (MAPKs), leading to an up-regulation of the pro-apoptotic protein Bax.¹⁴ Bax, in turn, stimulates the mitochondrial release of cytochrome c, activation of caspases, and ultimately cardiomyocyte apoptosis and cardiac remodelling (Figure 1).¹⁵ Furthermore, an increase in OS following DOX administration has been shown to disrupt myofibrillar and cytoskeletal structural integrity by down regulating alpha-myosin heavy chain, cardiac troponin I, desmin, and dystrophin.¹⁶ This is achieved through GATA-1 down-regulation and calpain activation.¹⁷⁻¹⁸ TRZ does not damage cardiomyocytes when used as a single agent.¹⁹ However, TRZ does potentiate DOX induced cardiac damage by a number of mechanisms including an increase in cardiomyocyte susceptibility to OS. This effect is achieved by altering apoptotic signalling pathways, specifically increasing the expression of the pro-apoptotic proteins Bcl-xS and Bax and decreasing anti-apoptotic Bcl-xL expression.²⁰ Ultimately, this disrupts mitochondrial function and triggers apoptosis through caspase activation. TRZ further contributes to DOX induced cardiotoxicity by preventing dimerization of the HER-2 receptor, which is essential for downstream signalling and cell survival.²¹

The central role of OS in the pathophysiology of DOX+TRZ mediated cardiotoxicity raises the question as to whether anti-oxidants could serve as cardioprotective agents in this setting. A number of anti-oxidants have been shown to reduce DOX toxicity, but are not without side effects.²²⁻²⁴ One such compound, N-acetylcysteine (NAC), a thiol-containing anti-oxidant, is able to replenish intracellular stores of reduced GSH and contribute to cellular redox regulation.²⁵⁻²⁶ Unverferth *et al.* randomized 20 patients to receive prophylactic NAC or placebo prior to a single injection of DOX for a variety of tumors.²⁷ Endomyocardial biopsies preformed at baseline, 4, and 24 hours demonstrated a DOX mediated change in tubular area and mitochondrial swelling within the myocardial tissue, which was not attenuated by the prophylactic administration of NAC.²⁷ NAC efficacy may be limited by its bioavailability as the hydrophilicity incurred by the negatively charged carboxyl moiety prevents intracellular accumulation.²⁵

In order to improve the bioavailability of NAC, a structural variant, N-acetylcysteine amide (NACA), was recently developed. NACA contains an amide moiety to promote lipophilicity, and thus intracellular accumulation.²⁵ Consequently, NACA was shown to be significantly more effective than NAC at restoring intracellular thiols and protecting against oxidation in tert-butylhydroperoxide treated red blood cells.²⁵ Furthermore, in an *in vitro* model, NACA attenuated DOX induced OS in embryonic rat cardiomyocytes, restoring the GSH/GSSG ratio, decreasing lipid peroxidation, and restoring the activity of enzymatic anti-oxidant defenses.²⁶ Despite these promising findings, the cardioprotective capabilities of NACA in an *in vivo* murine model of DOX+TRZ mediated cardiotoxicity remain unknown.

OBJECTIVE

To evaluate the potential cardioprotective role of the anti-oxidant NACA to mitigate the cardiotoxic side effects associated with DOX+TRZ therapy in an acute murine model of chemotherapy induced cardiotoxicity.

METHODS

A. ACUTE MURINE MODEL OF DOX+TRZ INDUCED CARDIOMYOPATHY

All animal procedures were conducted in accordance with guidelines published by the Canadian Council on Animal Care. All procedures, including drug administration and longitudinal echocardiographic studies, were approved by the Animal Protocol Review Committee at the University of Manitoba.

For the acute model of chemotherapy induced cardiomyopathy, a total of 100 WT C57Bl/6 female mice were randomized to one of the following regimens: (1) 0.9% saline (intraperitoneal (i.p.); n=5); (2) NACA (250 mg/kg, i.p.; n=5); (3) DOX (20 mg/kg, i.p.; n=15); (4) TRZ (10 mg/kg, i.p.; n=15); (5) DOX+TRZ (n=15); (6) NACA+DOX (n=15); (7) NACA+TRZ (n=15); and (8) NACA+DOX+TRZ (n=15) (Figure 2). Saline, DOX, and TRZ were administered at day 0 as a single injection; NACA was administered 30 minutes in advance for mice in the relevant treatment arms. The mice were euthanized after 10 days for assessment of OS and apoptosis (Figure 2). The cumulative doses of DOX or TRZ achieved were the minimum concentration to induce a chemotherapy mediated cardiomyopathy, as previously validated by our group and others.^{19,28}

A second protocol was conducted for histological analysis and to evaluate for early evidence of OS injury. A total of 70 female C57Bl/6 mice were randomized to the following treatment arms (1) Saline; (2) NACA; (3) DOX; (4) TRZ; (5) DOX+TRZ; (6) NACA+DOX (7) NACA+TRZ (8) NACA+DOX+TRZ (Figure 2). Saline, DOX, and TRZ were administered as a single injection at time 0; NACA was administered 30 minutes in advance for mice in the relevant treatment arms. The mice were euthanized after 72 hours for analysis.

B. MURINE ECHOCARIOGRAPHY

In vivo cardiac function was assessed at baseline and serially for 10 days by murine echocardiography. Images were acquired in awake mice using a 13-MHz probe (Vivid 7, GE Medical Systems, Milwaukee, WI, US). Mice were imaged in both the parasternal long and short axis views, as previously described.^{19,28} Echocardiographic parameters were calculated offline using the EchoPAC PC software (Vivid 7, version 11.2, GE Medical Systems, Milwaukee, WI, US).

The parasternal long axis view was used to trace left ventricular end systolic and end diastolic volumes and to calculate left ventricular ejection fraction (LVEF). M-mode echocardiography in the short axis view was used to measure LV cavity dimensions, including LV end-diastolic diameter (LVEDD), LV end-systolic diameter (LVESD), posterior wall thickness (PWT), interventricular septal thickness (IVS), as well as heart rate (HR). LV fractional shortening (FS) was calculated by the EchoPAC program.

C. HISTOLOGICAL ANALYSIS

A section of cardiac tissue was removed from euthanized mice and flash frozen in liquid nitrogen for histological analysis. Fixation with 3% glutaraldehyde in 0.1 M phosphate buffer (pH 7.3) was conducted for 3 hours at room temperature. The fixed tissue was then rinsed and buffered in 0.1 phosphate buffer with 5% sucrose for 24 hours at 4°C. 1% osmium tetroxide in 0.01 M phosphate buffer was used for post-fixation (2 hours). The tissue was dehydrated in ethanol of increasing concentration, embedded in Epon 812, and sectioned as previously described.²⁹ Tissue sections were stained with uranyl acetate and lead citrate and viewed using the Phillips CM12 electron microscope to evaluate cellular architecture.

D. OXIDATIVE STRESS (OS)

OS was assessed by quantifying phospholipid peroxidation and superoxide production. Lipids were extracted from cardiac tissue as previously described.³⁰ Briefly, frozen tissues were ground into a powder using liquid nitrogen. 6 ml C-M mixture (2:1 v/v, 0.01% BHT), 0.1 ml

internal standard, and 1.5 ml PBS were added. The solution was centrifuged at 3500 RPM for 5 minutes (4°C), after which the lipid phase was removed. 4.5 ml of C-M-PBS (86:14:1) was added to the remaining aqueous phase, which was centrifuged at 3500 RPM for 5 minutes (4°C) to repeat the extraction. The lipid phase was evaporated to dryness using a nitrogen evaporator. Lipid extracts were reconstituted in acetonitrile/isopropanol/water (65:30:5 v/v/v). Compounds were analyzed using high performance liquid chromatography (Shimadzu, USA MFG Inc) coupled to a 4000 QTrap Triple Quadrupole Linear Ion Trap Mass Spectrometer with a Turbo V electrospray ion source (Absciex, 500 Old Connecticut Path, Framingham MA 01701 USA). 0.03 ml lipid extract was injected onto an Ascentis Express C18 column (15cmx2.1mm, 2.7 µm; Supelco Analytical, Bellefonte, PA 16823-0048 USA) heated to 45°C. Elutions were performed via a linear gradient of solvent A (acetonitrile-water, 60:40 v/v) and solvent B (isopropanol-acetonitrile, 90:10 v/v), both of which contained 10 mM ammonium formate and 0.1% formic acid. The following gradient was used: 0.01 min: 32% B; 1.50 min: 32% B; 4.0 min: 45% B; 5.0 min: 52% B; 8.0 min: 58% B; 11.0 min: 55% B; 14.0 min: 70% B; 18.0 min: 76% B; 21.0 min: 97% B; 25.0 min: 97% B; 25.1 min: 32% B; and 30.0 min: 32% B. A flow rate of 0.26 ml/min was maintained throughout the analytical run. Data was quantified using Multiquant 2.1 software.

Superoxide production was quantified by lucigen-enhanced chemiluminescence.³¹ Cardiac tissue was incubated in Krebs-Hepes buffer with 10 µM NADPH and then transferred into a 96-well plate with 300 µl of Krebs-Hepes buffer, 10 µM NADPH, and 10 µM lucigenin. Data was collected by a multi-label counter for 60 seconds.

E. APOPTOSIS

Pro-apoptotic (PARP, caspase-3, Bax) and anti-apoptotic (Bcl-xL) protein expression was assessed by Western blot analysis.²⁸ Heart tissue was ground to a powder using liquid nitrogen and placed in radioimmunoprecipitation (RIPA) buffer containing protease and phosphatase inhibitors (Thermo Scientific). Samples were cooled for 20 minutes and then centrifuged at 10 000 RPM for 10 minutes (4°C). The resulting supernatant was removed and extracted proteins were quantified using the BioRad protein assay.

For the BioRad protein assay, 30 µg protein lysate was separated by 12% sodium dodecyl sulfate polyacrylamide gel (SDS-PAGE) at 100 V for 1.5 hours (Mini-PROTEAN Tetra System, BioRad). Proteins were then transferred onto a 0.45 µm PVDF membrane (Roche Diagnostics) for 2 hours at 100 V (4°C). After completion of the transfer, the membrane was blocked for 1 hour in BSA blocking buffer/TBST (Thermo Scientific). The membrane was then incubated with the appropriate primary polyclonal antibody (Cell Signaling Technology Inc.; Beverly, MA) for 24 hours at 4°C, washed and then incubated with goat anti-rabbit IgG secondary antibody (Bio-Rad; Hercules, CA) for 45 minutes. Bands were visualized using the ECL Plus Detection Reagent (Western Lighting Plus-ECL, Amersham) and X-ray film exposure. GAPDH polyclonal antibody was used as a loading control (Sigma). Band intensity was quantified using Quantity One analysis software (BioRad Laboratories, Inc).

F. STATISTICAL ANALYSIS

Statistical analysis was completed using SPSS 15.0 and Graphpad Prism 5 software. Data is expressed as a mean±SD with a p value of < 0.05 considered significant. Statistical significance of data obtained from echocardiographic analysis was determined using a mixed factorial design with repeated measurements for the factor of time. An ANOVA Post hoc analysis was completed for independent variables. Post hoc analysis for group variances was done with the Levene's test. Damage on histological analysis was graded in severity from 1 to 4 by an

observer blinded to the treatment groups; values were compared using the Mann-Whitney test. Significance of data from the biochemical and Western blot analyses was determined using a Student's-t test.

RESULTS

A. MURINE ECHOCARDIOGRAPHY

HR and PWT were similar between all mice at baseline and remained unchanged at day 10 in all treatment groups (Table 1). LV cavity dimensions were similar between all mice at baseline and remained unchanged at day 10 in the saline, NACA, TRZ, and NACA+TRZ groups (Table 1). DOX administration resulted in an increase in LVEDD from 3.2 ± 0.2 mm to 3.9 ± 0.2 mm at day 10 ($p < 0.05$). Similarly, LVEDD increased in the DOX+TRZ group from 3.2 ± 0.1 mm at baseline to 4.3 ± 0.2 mm by day 10 ($p < 0.05$). NACA prevented adverse cardiac remodelling at day 10, such that LVEDD was 3.4 ± 0.1 mm and 3.6 ± 0.1 mm for the NACA+DOX and NACA+DOX+TRZ groups, respectively ($p < 0.05$).

The LVEF was similar between all mice at baseline and remained unchanged by day 10 in the saline, NACA, TRZ, and NACA+TRZ groups (Table 1). In both DOX and DOX+TRZ treated mice, conventional echocardiographic indices showed a decrease in LVEF at day 10. In the DOX treatment arm, LVEF declined from $73 \pm 4\%$ at baseline to $43 \pm 2\%$ at day 10 ($p < 0.05$, Figure 3). Similarly, in the DOX+TRZ treatment arm, LVEF declined from $73 \pm 4\%$ at baseline to $32 \pm 2\%$ at day 10 ($p < 0.05$, Figure 3). Prophylactic NACA administration was cardioprotective, improving the LVEF at day 10 to $62 \pm 3\%$ and $55 \pm 3\%$ for NACA+DOX and NACA+DOX+TRZ treated mice, respectively ($p < 0.05$, Figure 3).

B. HISTOLOGICAL ANALYSIS

Histological integrity of the LV myocardium was preserved in mice treated with saline at the 72 hour time point. Myofibril degradation and vacuolization were visualized by electron microscopy in the cardiac tissue of mice treated with DOX+TRZ, representing architectural cardiac damage (Figure 4). Prophylactic NACA administration attenuated the degree of myocardial damage observed (Figure 4).

C. OXIDATIVE STRESS (OS)

OS was quantified by measuring lipid peroxidation in cardiac tissue obtained from mice in the 72 hour study. In control mice, fragmented oxidized phospholipids were quantified at 1.37 ng/mg. Levels were significantly increased at 4.81 ng/mg and 5.07 ng/mg for mice in the DOX and DOX+TRZ treatment arms, respectively ($p < 0.05$, Figure 5). The DOX+TRZ mediated increase in oxidized phospholipids was attenuated by prophylactic NACA administration. Fragmented oxidized phospholipids were significantly decreased to 2.62 ng/mg and 1.42 ng/mg for the NACA+DOX and NACA+DOX+TRZ groups, respectively ($p < 0.05$, Figure 5).

OS stress was further assessed by quantifying superoxide production for mice in the 10 day study. Superoxide production was amplified 3-fold and 4-fold in mice administered DOX and DOX+TRZ, respectively ($p < 0.05$; Figure 6). Following prophylactic treatment with NACA, superoxide production rates in the NACA+DOX and NACA+DOX+TRZ groups were significantly decreased and approached those quantified in the controls ($p < 0.05$; Figure 6).

D. APOPTOSIS

Markers of apoptotic (PARP, caspase-3, Bax) and anti-apoptotic (Bcl-xL) processes were evaluated in the cardiac tissue of mice from the 10 day study. PARP levels did not significantly differ from that of controls in any of the treatment groups. Caspase-3 levels in the DOX and DOX+TRZ groups were elevated 3- and 4-fold, respectively, as compared to control levels ($p < 0.05$, Figure 7). The prophylactic administration of NACA attenuated the rise in caspase-3. Caspase-3 levels in mice treated with NACA+DOX and NACA+DOX+TRZ were elevated 2.3- and 2.6-fold, respectively, as compared to control levels ($p < 0.05$, Figure 7). The ratio of the apoptotic protein Bax to the anti-apoptotic protein Bcl-xL (Bax/Bcl-xL) was elevated 1.5- and 1.9-fold in mice treated with DOX and DOX+TRZ, respectively, when normalized to saline controls ($p < 0.05$, Figure 8). Again, NACA attenuated the increase; a 1.3- and 1.4-fold elevation in Bax/Bcl-xL was observed for the NACA+DOX and NACA+DOX+TRZ groups ($p < 0.05$, Figure 8).

DISCUSSION

Although DOX+TRZ therapy constitutes the mainstay of breast cancer treatment, its efficacy is limited by a dose-related cardiotoxicity. This contributes significantly to the morbidity and mortality in the breast cancer population as approximately 1 in 4 women receiving DOX+TRZ therapy are at risk of developing chemotherapy induced cardiomyopathy.¹² Our increased understanding of the role of OS in the pathogenesis of DOX+TRZ mediated cardiotoxicity in conjunction with the recent development of the potent anti-oxidant NACA, warrants investigating the cardioprotective properties of this novel agent in the breast cancer setting. The current study used an acute murine model of chemotherapy induced cardiomyopathy in order to evaluate the cardioprotective effects of NACA in the prevention of DOX+TRZ mediated cardiotoxicity. We demonstrated NACA to be partially cardioprotective by i) attenuating adverse cardiovascular remodelling on echocardiography; ii) preserving cardiac architecture upon histological analysis of cardiac tissue; iii) decreasing OS, as quantified by oxidized phospholipid and superoxide production; and iv) attenuating levels of apoptosis. These findings suggest a potential for the prophylactic use of NACA in the prevention of DOX+TRZ mediated cardiotoxicity in the breast cancer setting.

The cardiotoxic side effects of DOX and DOX+TRZ have been previously validated in both acute and chronic murine models.^{19,28,31} Neilan *et al.* evaluated the cardiotoxic side effects of DOX in an acute murine model of chemotherapy induced cardiotoxicity. Wild-type mice that received a single dose of 20 mg/kg DOX developed LV cavity dilatation with LV systolic dysfunction over a 14 day period.³¹ A similar study by Jassal *et al.* characterized the combined cardiotoxic side effects of DOX (20 mg/kg)+TRZ (10 mg/kg) administration in a murine model.²⁸ By day 4 of treatment with DOX+TRZ, mice demonstrated progressive LV dilatation and systolic dysfunction.²⁸ The present study corroborates these findings. Murine echocardiography revealed LV cavity dilatation and systolic dysfunction in mice administered DOX alone over a 10 day period. This effect was further potentiated by the concomitant administration of TRZ, illustrating the synergistic effect of TRZ on DOX mediated cardiotoxicity. In the current study, we demonstrated for the first time the prophylactic use of NACA in attenuating the cardiotoxic side effects of DOX and DOX+TRZ. Both LVEDD and LVEF values were significantly improved in the NACA+DOX and NACA+DOX+TRZ treatment arms. This finding indicates that NACA possesses cardioprotective capabilities against DOX+TRZ mediated cardiotoxicity.

Endomyocardial biopsy and subsequent histological analysis of cardiac tissue is the most sensitive and specific modality to detect chemotherapy induced cardiomyopathy.⁴ However, its use in clinical practice is largely replaced by imaging, as a result of the invasive nature of cardiac

biopsies as a diagnostic procedure. Histological analysis, however, remains a useful technique to evaluate the degree of cardiac remodelling in animal models of chemotherapy mediated cardiomyopathy. Characteristic histological findings in cardiac tissue from mice treated with DOX include myofibril loss, sarcoplasmic reticulum distension, cytoplasmic vacuolization, mitochondrial swelling, and an increase in lysosomal number.^{4,28,32} Jassal *et al.* demonstrated vacuolization and cytoplasmic clearing in mice treated with a single dose of 20 mg/kg DOX by day 5 of the study, which was potentiated by TRZ treatment.²⁸ The current study demonstrated findings consistent with classic structural changes observed in DOX+TRZ mediated cardiomyopathy. Histological analysis of cardiac tissue from mice in the 72 hour protocol demonstrated myofibril degradation and vacuolization in the DOX+TRZ treatment arm. Corroborating our echocardiographic findings, the prophylactic administration of NACA attenuated the degree of cardiac damage observed by electron microscopy, further supporting the protective benefits afforded by NACA against DOX+TRZ cardiomyopathy.

Elucidating the mechanistic pathway by which DOX+TRZ promotes cardiac damage is imperative in order to develop strategies to interfere with the process. A number of hypotheses exist in an attempt to explain the cardiotoxic side effects of DOX therapy. These include nucleic acid and protein inhibition, release of vasoactive amines, mitochondrial dysfunction, and myocardial electrolyte imbalances.¹³ OS is suspected to play a central role in the pathogenesis of DOX mediated cardiotoxicity and as such, is well characterized in the literature. The molecular structure of DOX, namely the presence of a quinone ring, lends itself to the production of reactive oxygen species. Once intracellular, DOX can complex with mitochondria, permitting the respiratory chain enzyme NADPH dehydrogenase to act as a catalyst, converting the quinone ring in DOX to a semiquinone.³³ The electrons generated from this process are capable of reducing molecular oxygen to generate free radical species and OS.¹³ Thornalley *et al.* demonstrated an increase in cellular OS following DOX administration in an *in vitro* model.³⁴ Hydroxyl radicals were detected by electron spin resonance in rat myocardial sarcosomes treated with 100 μ M DOX.³⁴ The present study supports this finding, as superoxide production, a marker of OS, was increased 3-fold in mice treated with DOX. We further demonstrated that concomitant TRZ therapy potentiates the generation of OS, as superoxide production was increased 4-fold in mice administered combination DOX+TRZ. Prophylactic NACA attenuated OS production such that superoxide levels approached those of controls. The ability of NACA to improve systolic function and decrease OS further supports the importance of OS in the pathogenesis of DOX+TRZ mediated cardiomyopathy. In addition, it illustrates the cardioprotective capacity of NACA in this setting, by way of modulating OS (Figure 1).

Reactive oxygen species oxidize unsaturated lipids in plasma membranes to generate lipid peroxides, ultimately damaging cellular barriers.^{32,35} The peroxidation of lipids is emerging as an important player in the pathogenesis of cardiovascular disease, and studies have demonstrated direct toxic effects on cardiomyocytes. The addition of 4-hydroxy-2-nonenal, a major product of lipid peroxidation, to cardiomyocytes stimulates the generation of reactive oxygen species, a rise in intracellular calcium and cellular hypercontracture.³⁶ Myers *et al.* quantified malondialdehyde, a marker of lipid peroxidation, in mice treated with DOX.³⁵ Although malondialdehyde was not detected in cardiac tissue from control mice, it was readily detected in DOX treated mice, reaching its peak concentration 4 days following administration of the drug.³⁵ In the current study, there was a significant increase in oxidized phospholipids in mice treated with either DOX or DOX+TRZ. NACA attenuated lipid peroxidation in both the NACA+DOX and NACA+DOX+TRZ treatment arms, again suggesting that NACA interferes with OS production, which is a necessary intermediate in the pathogenesis of cardiac disease.

OS and reactive oxygen species ultimately trigger apoptotic pathways in cardiomyocytes. A number of previous studies have demonstrated the induction of a pro-apoptotic environment following DOX+TRZ administration in cardiomyocytes. Previously, Kumar *et al.* exposed cardiomyocytes to 20 μ M DOX, and subsequently observed cellular morphological changes and an increased number of apoptotic myocytes and nucleosomal fragmentation by TUNEL assay.³⁷ TRZ similarly alters cellular apoptotic milieu, specifically by modifying apoptotic Bcl-xS, Bax, and anti-apoptotic Bcl-xL expression.²⁰ Consequently, the combination treatment of DOX+TRZ induces apoptosis, as demonstrated by PARP cleavage, and an increased ratio of p17/p32 which signifies caspase 3 activation, a downstream initiator of apoptosis.²⁸ The current study supports these findings; an increased Bax/Bcl-xL ratio and caspase 3 expression was observed in both the DOX and DOX+TRZ treatment arms. We further demonstrated the ability of NACA to attenuate the level of apoptosis in mice treated with DOX or DOX+TRZ, normalizing the Bax/Bcl-xL ratio and caspase 3 values. This finding further supports the growing evidence that NACA possesses cardioprotective capabilities in the setting of DOX+TRZ mediated cardiomyopathy.

The mechanisms underlying DOX+TRZ anti-tumor and cardiotoxic effects differ, prompting the search for a cardioprotective agent that solely interferes with the latter mechanism. Previous basic science and clinical studies have investigated the cardioprotective benefit provided by a number of agents in the setting of DOX+TRZ cardiomyopathy, including dexrazoxane, angiotensin converting enzyme inhibitors (ACEi), beta-blockers, and anti-oxidants. Dexrazoxane is a derivative of EDTA, able to chelate iron and prevent the generation of free radicals.⁷ Dexrazoxane is FDA approved for women with metastatic breast cancer who have received a cumulative dose of 300 mg/mg² of DOX, and was also employed in pediatric clinical trials of acute lymphoblastic lymphoma and acute myelogenous lymphoma.⁶ Reports that dexrazoxane may increase the incidence of acute myelogenous lymphoma/myelodysplastic syndromes and second malignant neoplasms²³ have not been replicated in subsequent studies.³⁸ Despite this, caution must be exercised when prescribing dexrazoxane because of the potential risk for secondary malignancies, as well as, myelosuppression.

ACEi and beta-blockers are class I recommended agents for use in heart failure patients with reduced LVEF, and as such are considered as first line treatment after the development of DOX+TRZ mediated cardiomyopathy.³⁹ Studies have suggested a role for the renin angiotensin system (RAS) in DOX mediated cardiotoxicity. Angiotensin II type 1a receptor knockout mice failed to develop DOX induced cardiac dysfunction, myofibrillar loss and apoptosis in both acute and chronic murine models.⁴⁰ As such, a number of animal models have demonstrated a benefit afforded by prophylactic ACEi in the setting of DOX induced cardiomyopathy.⁴¹⁻⁴² Boucek *et al.* demonstrated the cardioprotective effects of daily lisinopril for 10 weeks following the administration of 2 mg/kg DOX in a chronic rabbit model of chemotherapy induced cardiomyopathy.⁴¹ Lisinopril treatment attenuated DOX induced cardiomyocyte loss and ventricular pro-atrial natriuretic peptide (ANP) expression, a marker of RAS activation.⁴¹ Similarly, Abd El-Aziz *et al.* evaluated the administration of captopril (10 mg/kg) or enalapril (2 mg/kg) for 7 days prior to intraperitoneal injection of 15 mg/kg DOX in rats.⁴² Pre-treatment with ACEi reduced lipid peroxidation and decreased serum markers of cardiotoxicity, such as creatine kinase isoenzyme.⁴² These basic clinical science studies have recently been translated to the clinical arena. The OVERCOME trial involved 90 patients with acute leukemia or malignant hemopathies randomized to receive an ACEi (enalapril) and beta-blocker (carvedilol) or control.⁴³ The combination treatment of ACEi and beta-blockade resulted in a lower rate of death, heart failure, or LVEF <45%.⁴³ The ongoing MANTICORE study randomized 159 patients with HER-2 positive breast cancer to receive ACEi (perindopril), beta-blocker (bisoprolol) or placebo 1 week prior to TRZ therapy.⁴⁴ The results of the MANTICORE trial will aid in the

prescriptions of prophylactic ACEi or beta-blockers in the setting of DOX+TRZ induced cardiotoxicity.

The central role of OS in the pathogenesis of DOX+TRZ mediated cardiac dysfunction has provoked investigations to determine the efficacy of anti-oxidants, such as probucol, and NAC, as cardioprotective agents. Prophylactic probucol (15 mg/kg for 2 weeks) decreased mortality from >80% to 40%, in addition to attenuating histological and biochemical markers of damage in an acute murine model of DOX+TRZ induced cardiotoxicity.¹⁹ However, probucol may alter the pharmacokinetics of DOX therapy, and as a consequence interfere with anti-tumor activity. One study demonstrated an increase in plasma DOX clearance, increased hepatic/renal and reduced splenic concentrations of DOX.²² This issue is contended in the literature, as the anti-tumor efficacy of DOX in combination with prophylactic probucol was equivalent to that of the DOX only group in a murine model of lymphoma; DOX versus DOX+probucol treatment did not significantly affect tumor size.⁴⁵ The cardioprotective capability of NAC was demonstrated in 25 rabbits with echocardiography-confirmed DOX induced cardiomyopathy.⁴⁶ 13 rabbits received prophylactic treatment with 300 mg/kg NAC daily for 4 weeks, while 12 controls received normal saline at this time.⁴⁶ NAC improved the total anti-oxidative capacity, GSH levels, Bcl-2/Bax ratio and decreased apoptosis, ultimately improving cardiac function.⁴⁶ These results contrast previous studies which failed to demonstrate a cardioprotective effect, likely as a result of the large cumulative dose of NAC employed.²⁷ However, high dose NAC, which appears necessary to achieve cardioprotective effect, is typically associated with toxic side effects such as ammonia production and suppression of respiratory bursts.²⁴

We have attempted, with the use of NACA, to address the limitations encountered in previous studies, namely toxicity and modulation of DOX+TRZ anti-tumor efficacy. The efficacy of NACA was demonstrated in an *in vitro* model of chemotherapy induced cardiotoxicity. Shi *et al.* demonstrated the ability of NACA to attenuate reactive oxygen species production, lipid peroxidation and increase the GSH/GSSG ratio in cardiomyocytes.²⁶ We have demonstrated for the first time in an *in vivo* model of chemotherapy induced cardiomyopathy, the ability of NACA to protect against structural and functional cardiac damage. It remains to be determined whether NACA interferes with DOX+TRZ anti-tumor efficacy, and future studies are warranted.

There are a number of limitations in the current study. An acute murine model of chemotherapy induced cardiotoxicity was employed in order to evaluate the efficacy of NACA as a cardioprotective agent. However, chemotherapeutic treatments are administered over longer periods of time; breast cancer regimens typically consist of 4, 21 day cycles.⁴⁷ In addition, TRZ is administered after anthracycline chemotherapy in the clinical setting and is continued for 1 year.⁴⁷ It would therefore be of use to evaluate the cardioprotective efficacy of NACA in a chronic animal model that more closely emulates the chemotherapeutic regimen employed in the breast cancer population. Furthermore, we did not evaluate the anti-tumor efficacy of DOX+TRZ treatment when combined with NACA on breast cancer cells. This is an important consideration as the ultimate goal is to develop a cardioprotective agent that does not affect the anti-tumor action of DOX+TRZ. It will be worthwhile to include this component in future studies.

CONCLUSION

The significant cardiotoxicity associated with breast cancer chemotherapy necessitates the development of cardioprotective strategies. We demonstrated for the first time in a murine model of chemotherapy induced cardiomyopathy, the ability of NACA to mitigate structural and functional damage associated with DOX+TRZ therapy. Clinical studies are warranted to

translate these basic science findings into the clinical arena and ultimately achieve the goal of decreasing morbidity and mortality in the breast cancer population.

REFERENCES

1. Canadian Cancer Society's Advisory Committee on Cancer Statistics. *Canadian Cancer Statistics 2015*. Toronto, ON: Canadian Cancer Society; 2015.
2. Gottlieb JA, Rivkin SE, Spigel SC, et al. Proceedings: Superiority of adriamycin over oral nitrosoureas in patients with advanced breast carcinoma. A Southwest Cancer Chemotherapy study Group study. *Cancer* 1974 Feb;33(2):519-26.
3. Kaklamani VG, Gradishar WJ. Adjuvant Therapy of Breast Cancer. *Cancer Invest* 2005;23(6):548-60.
4. Singal PK, Iliskovic N. Doxorubicin-induced cardiomyopathy. *N Engl J Med* 1998 Sep 24;339(13):900-5.
5. Lefrak EA, Pitha J, Rosenheim S, et al. A clinicopathologic analysis of adriamycin cardiotoxicity. *Cancer* 1973;32(2):302-14.
6. Raj S, Franco VI, Lipshultz SE. Anthracycline-induced cardiotoxicity: a review of pathophysiology, diagnosis, and treatment. *Curr Treat Options Cardiovasc Med* 2014;16:315.
7. Ludke AR, Al-Shudiefat AA, Dhingra S, et al. A concise description of cardioprotective strategies in doxorubicin-induced cardiotoxicity. *Can J Physiol Pharmacol* 2009;87:756-63.
8. Slamon DJ, Clark GM, Wong SG, et al. Human breast cancer: correlation of relapse and survival with amplification of the HER-2/neu oncogene. *Science* 1987;235(4785):177-82.
9. Romond EH, Perez EA, Bryant J, et al. Trastuzumab plus adjuvant chemotherapy for operable HER2-positive breast cancer. *N Engl J Med* 2005;353(16):1673-84.
10. Perez EA, Romond EH, Suman VJ, et al. Trastuzumab plus adjuvant chemotherapy for human epidermal growth factor receptor 2-positive breast cancer: planned joint analysis of overall survival from NSABP B-31 and NCCTG N9831. *J Clin Oncol* 2014;32(33):3744-52.
11. Slamon DJ, Leyland-Jones B, Shak S, et al. Use of chemotherapy plus a monoclonal antibody against HER2 for metastatic breast cancer that overexpresses HER2. *New Eng J Med* 2001;344(11):783-92.
12. Wadhwa D, Fallah-Rad N, Grenier D, et al. Trastuzumab mediated cardiotoxicity in the setting of adjuvant chemotherapy for breast cancer: a retrospective study. *Breast Cancer Res Treat* 2009;117(2):357-64.
13. Singal PK, Iliskovic N, Li T, et al. Adriamycin cardiomyopathy: pathophysiology and prevention. *FASEB J* 1997;11(12):931-6.
14. Lou H, Kaur K, Sharma AK, et al. Adriamycin-induced oxidative stress, activation of MAP kinases and apoptosis in isolated cardiomyocytes. *Pathophysiology* 2006;13(2):103-9.
15. Finucane DM, Bossy-Wetzel E, Waterhouse NJ, et al. Bax-induced caspase activation and apoptosis via cytochrome c release from mitochondria is inhibitable by Bcl-xL. *J Biol Chem* 1999;274(4):2225-33.
16. Ito H, Miller SC, Billingham ME, et al. Doxorubicin selectively inhibits muscle gene expression in cardiac muscle cells in vivo and in vitro. *Proc Natl Acad Sci U S A* 1990;87(11):4275-9.
17. Meganathan K, Sotiriadou I, Natarajan K, et al. Signaling molecules, transcription growth factors and other regulators revealed from in-vivo and in-vitro models for the regulation of cardiac development. *Int J Cardiol.* 2015 Mar 15;183:117-28.
18. Lim CC, Zuppinger C, Guo X, et al. Anthracyclines induce calpain-dependent titin proteolysis and necrosis in cardiomyocytes. *J Biol Chem* 2004;279(9):8290-9.
19. Walker JR, Sharma A, Lytwyn M, et al. The cardioprotective role of probucol against anthracycline and trastuzumab-mediated cardiotoxicity. *J Am Soc Echocardiogr* 2011;24(6):699-705.

20. Grazette LP, Boecker W, Matsui T, et al. Inhibition of ErbB2 causes mitochondrial dysfunction in cardiomyocytes: implications for herceptin-induced cardiomyopathy. *J Am Coll Cardiol* 2004;44(11):2231-8.
21. Kulhari H, Pooja D, Rompicharla SV, Sistla R, et al. Biomedical Applications of Trastuzumab: As a Therapeutic Agent and a Targeting Ligand. *Med Res Rev*. 2015 Jul;35(4):849-76.
22. El-Demerdash E, Ali AA, Sayed-Ahmed MM, et al. New aspects in probucol cardioprotection against doxorubicin-induced cardiotoxicity. *Cancer Chemother Pharmacol* 2003;52(5):411-6.
23. Tebbi CK, London WB, Friedman D, et al. Dexrazoxane-associated risk for acute myeloid leukemia/myelodysplastic syndrome and other secondary malignancies in pediatric Hodgkin's disease. *J Clin Oncol* 2007;25(5):493-500.
24. Sunitha K, Hemshekhar M, Thushara RM, et al. N-Acetylcysteine amide: a derivative to fulfill the promises of N-Acetylcysteine. *Free Radic Res*. 2013 May;47(5):357-67.
25. Grinberg L, Fibach E, Amer J, et al. N-acetylcysteine amide, a novel cell-permeating thiol, restores cellular glutathione and protects human red blood cells from oxidative stress. *Free Radic Biol Med* 2005;38(1):136-45.
26. Shi R, Huang CC, Aronstam RS, et al. N-acetylcysteine amide decreases oxidative stress but not cell death induced by doxorubicin in H9c2 cardiomyocytes. *BMC Pharmacol* 2009;9:7.
27. Unverferth DV, Jagadeesh JM, Unverferth BJ, et al. Attempt to prevent doxorubicin-induced acute human myocardial morphologic damage with acetylcysteine. *J Natl Cancer Inst* 1983;71(5):917-20.
28. Jassal DS, Han SY, Hans C, et al. Utility of tissue Doppler and strain rate imaging in the early detection of Trastuzumab and anthracycline mediated cardiomyopathy. *J Am Soc Echocardiogr* 2009;22(4):418-24.
29. Luft JH. Improvements in epoxy resin embedding methods. *J Biophys Biochem Cytol* 1961;9:409-14.
30. Gruber F, Bicker W, Oskolkova OV, et al. A simplified procedure for semi-targeted lipidomic analysis of oxidized phosphatidylcholines induced by UVA irradiation. *J Lipid Res* 2012;53(6):1232-42.
31. Neilan TG, Blake SL, Ichinose F, et al. Disruption of nitric oxide synthase 3 protects against the cardiac injury, dysfunction, and mortality induced by Doxorubicin. *Circulation* 2007;116(5):506-14.
32. Singal PK, Li T, Kumar D, et al. Adriamycin-induced heart failure: mechanism and modulation. *Mol Cell Biochem* 2000;207(1-2):77-86.
33. Pacher P, Beckman JS, Liaudet L. Nitric oxide and peroxynitrite in health and disease. *Physiol Rev* 2007;87(1):315-424.
34. Thornalley PJ, Dodd NJ. Free radical production from normal and adriamycin-treated rat cardiac sarcosomes. *Biochem Pharmacol* 1985;34(5):669-74.
35. Myers CE, McGuire WP, Liss RH, et al. Adriamycin: the role of lipid peroxidation in cardiac toxicity and tumor response. *Science* 1977;197(4299):165-7.
36. Nakamura K, Miura D, Kusano KF, et al. 4-Hydroxy-2-nonenal induces calcium overload via the generation of reactive oxygen species in isolated rat cardiac myocytes. *J Card Fail* 2009;15(8):709-16.
37. Kumar D, Kirshenbaum L, Li T, et al. Apoptosis in isolated adult cardiomyocytes exposed to adriamycin. *Ann N Y Acad Sci* 1999;874:156-68.
38. Vrooman LM, Neuberg DS, Stevenson KE, et al. The low incidence of secondary acute myelogenous leukaemia in children and adolescents treated with dexrazoxane for acute lymphoblastic leukaemia: a report from the Dana-Farber Cancer Institute ALL Consortium. *Eur J Cancer* 2011;47(9):1373-9.
39. Yancy CW, Jessup M, Bozkurt B, et al. 2013 ACCF/AHA guideline for the management of heart failure: executive summary: a report of the American College of Cardiology

- Foundation/American Heart Association Task Force on practice guidelines. *Circulation* 2013;128(16):1810-52.
40. Toko H, Oka T, Zou Y, et al. Angiotensin II type 1a receptor mediates doxorubicin-induced cardiomyopathy. *Hypertens Res* 2002;25(4):597-603.
41. Boucek RJ Jr, Steele A, Miracle A, et al. Effects of angiotensin-converting enzyme inhibitor on delayed-onset doxorubicin-induced cardiotoxicity. *Cardiovasc Toxicol* 2003;3(4):319-29.
42. Abd El-Aziz MA, Othman AI, Amer M, et al. Potential protective role of angiotensin-converting enzyme inhibitors captopril and enalapril against adriamycin-induced acute cardiac and hepatic toxicity in rats. *J Appl Toxicol* 2001;21(6):469-73.
43. Bosch X, Rovira M, Sitges M et al. Enalapril and carvedilol for preventing chemotherapy-induced left ventricular systolic dysfunction in patients with malignant hemopathies: the OVERCOME trial (preventiOn of left Ventricular dysfunction with Enalapril and caRvedilol in patients submitted to intensive ChemOtherapy for the treatment of Malignant hEmopathies). *J Am Coll Cardiol* 2013;61(23):2355-62.
44. Pituskin E, Haykowsky M, Mackey JR, et al. Rationale and design of the Multidisciplinary Approach to Novel Therapies in Cardiology Oncology Research Trial (MANTICORE 101--Breast): a randomized, placebo-controlled trial to determine if conventional heart failure pharmacotherapy can prevent trastuzumab-mediated left ventricular remodeling among patients with HER2+ early breast cancer using cardiac MRI. *BMC Cancer* 2011;11:318.
45. Siveski-Iliskovic N, Hill M, Chow DA, et al. Probucol protects against adriamycin cardiomyopathy without interfering with its antitumor effect. *Circulation* 1995;91(1):10-5.
46. Wu XY, Luo AY, Zhou YR, et al. N-acetylcysteine reduces oxidative stress, nuclear factor- κ B activity and cardiomyocyte apoptosis in heart failure. *Mol Med Rep* 2014;10:615-24.
47. Bourdeanu L, Liu EA. Systemic treatment for breast cancer: chemotherapy and biotherapy agents. *Semin Oncol Nurs* 2015;31(2):156-62.

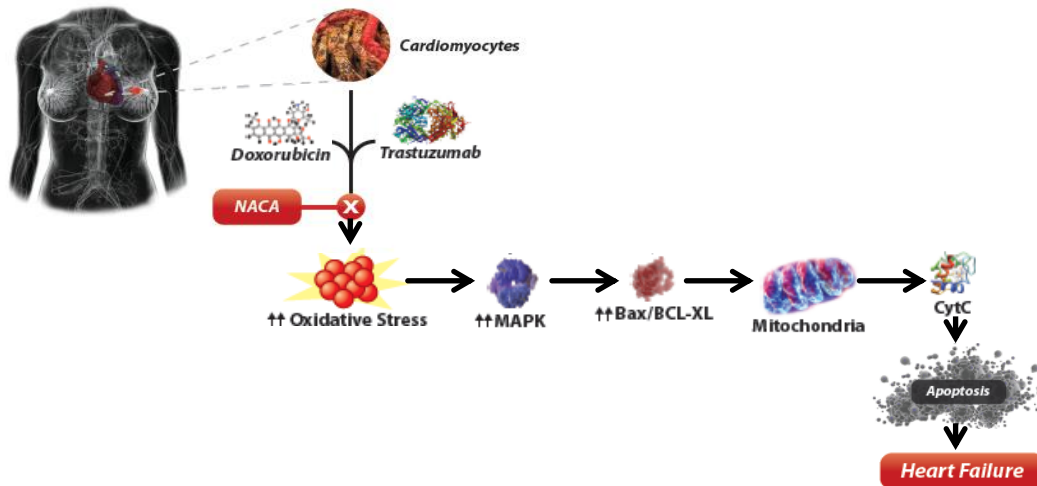


Figure 1: Illustration of the role of oxidative stress (OS) in the activation of the mitogen-activated protein kinase (MAPK) pathway leading to cardiomyocyte apoptosis.

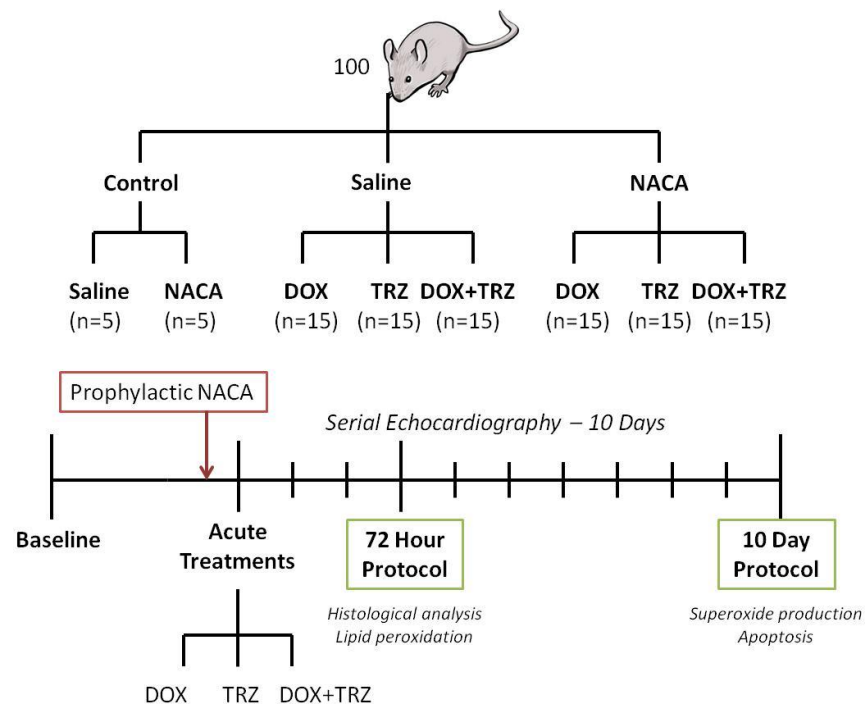


Figure 2: Experimental protocol: 100 WT C57Bl/6 female mice were randomized to one of the following regimens: (1) 0.9% saline (intraperitoneal (i.p.); n=5); (2) NACA (250 mg/kg, i.p.; n=5); (3) DOX (20 mg/kg, i.p.; n=15); (4) TRZ (10 mg/kg, i.p.; n=15); (5) DOX+TRZ (n=15); (6) NACA+DOX (n=15); (7) NACA+TRZ (n=15); and (8) NACA+DOX+TRZ (n=15). NACA was administered 30 minutes prior to the acute treatments. For the 72 hour protocol, mice were euthanized after 72 hours for histological analysis and determination of lipid peroxidation. For the 10 day protocol, daily echocardiography was conducted, after which mice were euthanized for detection of superoxide production and markers of apoptosis.

Echo Variable	Group	Baseline	Day 10	P-Value
HR (beats/min)	Saline	694±8	683±9	0.82
	NACA	675±11	690±10	0.78
	DOX	687±12	682±5	0.77
	NACA+DOX	689±10	691±8	0.65
	TRZ	705±15	702±11	0.86
	NACA+TRZ	704±12	695±9	0.87
	DOX+TRZ	701±8	689±12	0.78
	NACA+DOX+TRZ	688±11	693±7	0.70
PWT (mm)	Saline	0.81±0.02	0.82±0.01	0.83
	NACA	0.80±0.01	0.82±0.02	0.86
	DOX	0.82±0.02	0.82±0.01	0.91
	NACA+DOX	0.83±0.02	0.82±0.03	0.82
	TRZ	0.81±0.02	0.81±0.01	0.83
	NACA+TRZ	0.80±0.01	0.80±0.02	0.85
	DOX+TRZ	0.82±0.03	0.82±0.04	0.92
	NACA+DOX+TRZ	0.81±0.02	0.80±0.02	0.80
LVEDD (mm)	Saline	3.2±0.1	3.1±0.2	0.89
	NACA	3.1±0.1	3.2±0.1	0.76
	DOX	3.2±0.2	3.9±0.2*	<0.05
	NACA+DOX	3.1±0.1	3.4±0.1* [#]	<0.05
	TRZ	3.1±0.2	3.2±0.2	0.76
	NACA+TRZ	3.1±0.2	3.2±0.2	0.82
	DOX+TRZ	3.2±0.1	4.3±0.2*	<0.05
	NACA+DOX+TRZ	3.2±0.2	3.6±0.1* [#]	<0.05
LVEF (%)	Saline	72±4	73±4	0.87
	NACA	74±2	73±1	0.82
	DOX	73±4	43±2*	<0.05
	NACA+DOX	73±4	62±3* [#]	<0.05
	TRZ	71±4	72±3	0.88
	NACA+TRZ	73±4	73±1	0.68
	DOX+TRZ	73±4	32±2*	<0.05
	NACA+DOX+TRZ	72±4	55±3* [#]	<0.05

Table 1: Echocardiographic findings at baseline and day 10 in C57Bl/6 female mice receiving one of the drug regimens listed. Analyses included assessment of heart rate (HR), posterior wall thickness (PWT), left ventricular end-diastolic diameter (LVEDD), and left ventricular ejection fraction (LVEF). Values presented are mean±SEM. n=5 Saline; n=5 NACA; n=15 DOX; n=15 NACA+DOX; n=15 TRZ; n=15 NACA+TRZ; n=15 DOX+TRZ; n=15 NACA+DOX+TRZ. * p<0.05 Saline vs. treatment group. [#] p<0.05 DOX vs. NACA+DOX and DOX+TRZ vs. NACA+DOX+TRZ.

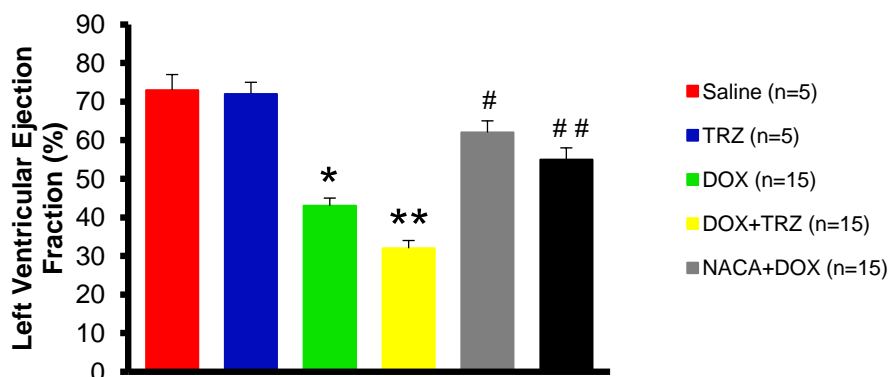


Figure 3: LV ejection fraction calculated in mice 10 days following administration with (1) saline; (2) TRZ; (3) DOX; (4) DOX+TRZ; (5) NACA+DOX; (6) NACA+DOX+TRZ. In the DOX and DOX+TRZ treatment arms, LVEF declined to $43 \pm 2\%$ and $32 \pm 2\%$. Prophylactic NACA improved the LVEF for DOX and DOX+TRZ treated mice to $62 \pm 3\%$ and $55 \pm 3\%$, respectively. * $p < 0.05$ Saline vs. DOX, ** $p < 0.05$ Saline vs. DOX+TRZ, # $p < 0.05$ DOX vs. NACA+DOX, ## $p < 0.05$ DOX+TRZ vs. NACA+DOX+TRZ.

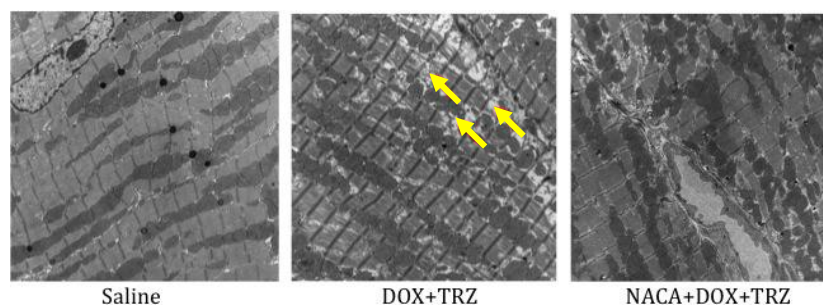


Figure 4: Histological analysis by electron microscopy of cardiac tissue obtained from mice in the saline, DOX+TRZ and NACA+DOX+TRZ treatment arms. Myofibril degradation and vacuolization was observed in mice treated with DOX+TRZ but attenuated by prophylactic NACA administration.

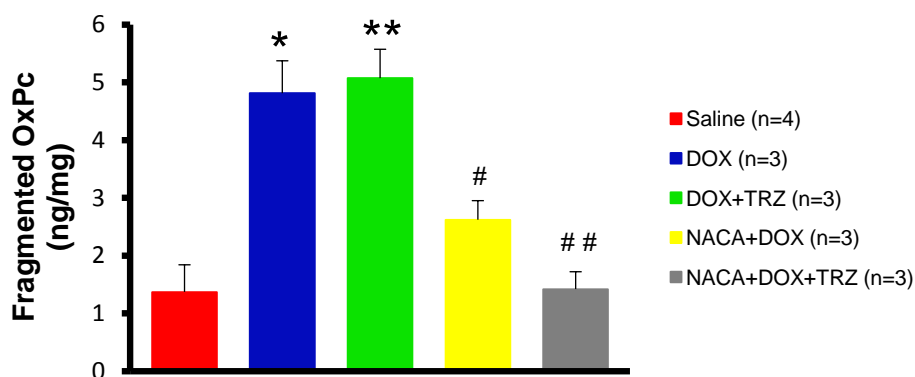


Figure 5: Oxidized phospholipids at 72 hours in mice treated with: (1) Saline; (2) DOX; (3) DOX+TRZ; (4) NACA+DOX; and (5) NACA+DOX+TRZ. Oxidized phospholipids were elevated in mice administered DOX and DOX+TRZ, which was attenuated by prophylactic NACA treatment. * $p < 0.05$ Saline vs. DOX, ** $p < 0.05$ Saline vs. DOX+TRZ, # $p < 0.05$ DOX vs. NACA+DOX, ## $p < 0.05$ DOX+TRZ vs. NACA+DOX+TRZ.

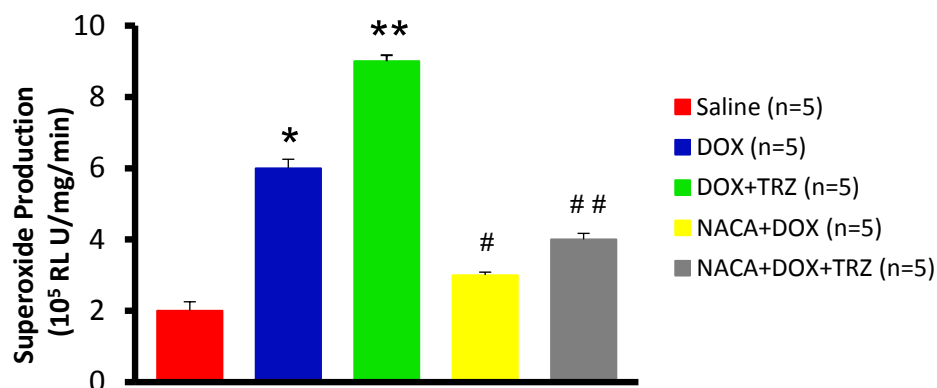


Figure 6: Cardiac superoxide production at day 10 in mice treated with: (1) Saline; (2) DOX; (3) DOX+TRZ; (4) NACA+DOX; and (5) NACA+DOX+TRZ. Superoxide production was amplified in mice administered DOX and DOX+TRZ, which was attenuated by prophylactic NACA treatment. * $p < 0.05$ Saline vs. DOX, ** $p < 0.05$ Saline vs. DOX+TRZ, # $p < 0.05$ DOX vs. NACA+DOX, ## $p < 0.05$ DOX+TRZ vs. NACA+DOX+TRZ.

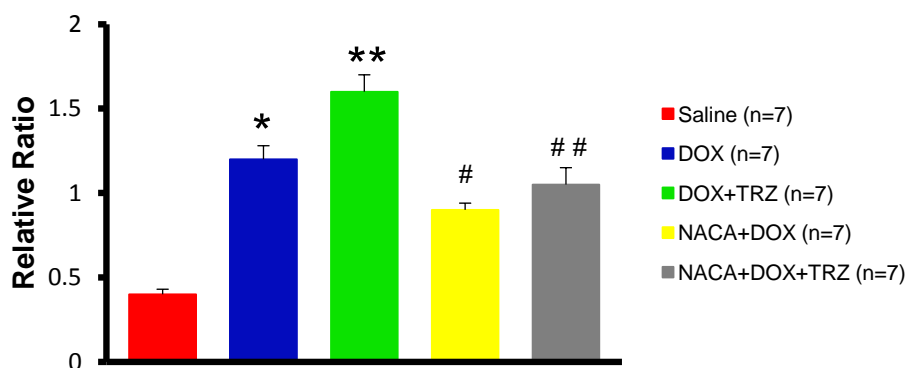


Figure 7: Caspase-3 levels in cardiac tissue at day 10 in mice treated with: (1) Saline; (2) DOX; (3) DOX+TRZ; (4) NACA+DOX; and (5) NACA+DOX+TRZ. Caspase-3 was elevated in the DOX and DOX+TRZ treatment arms. Prophylactic NACA attenuated caspase-3 levels. * $p < 0.05$ Saline vs. DOX, ** $p < 0.05$ Saline vs. DOX+TRZ, # $p < 0.05$ DOX vs. NACA+DOX, ## $p < 0.05$ DOX+TRZ vs. NACA+DOX+TRZ.

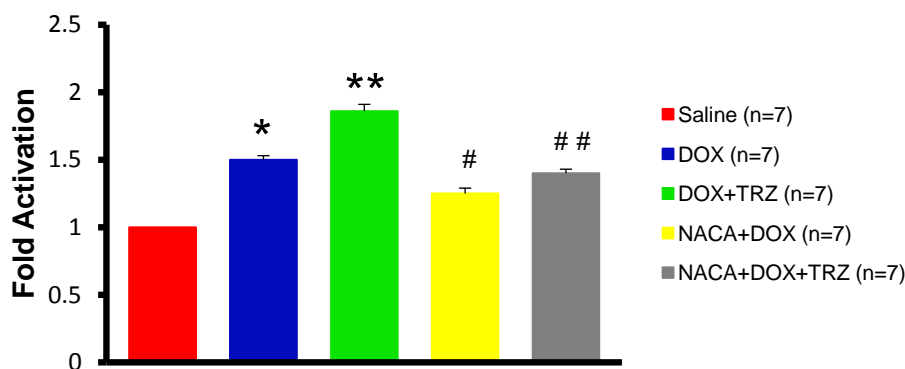


Figure 8: Bax/Bcl-xL ratio normalized to saline controls at day 10 in mice treated with: (1) Saline; (2) DOX; (3) DOX+TRZ; (4) NACA+DOX; and (5) NACA+DOX+TRZ. Bax/Bcl-xL was elevated in the DOX and DOX+TRZ treatment arms, which was attenuated by the administration of prophylactic NACA. * $p < 0.05$ Saline vs DOX, ** $p < 0.05$ Saline vs DOX+TRZ, # $p < 0.05$ DOX vs NACA+DOX, ## $p < 0.05$ DOX+TRZ vs NACA+DOX+TRZ.